PCCP

Accepted Manuscript

ROYAL SOCIETY OF CHEMISTRY

www.rsc.org/pccp

Journal Name

RSCPublishing

ARTICLE

How protein structure affects redox reactivity: example of Human centrin 2.

Cite this: DOI: 10.1039/xoxxoooooox

Abdeslam Et Taouil[a,e], Emilie Brun[b], Patricia Duchambon[c], Yves Blouquit[d], Manon Gilles[b], Emmanuel Maisonhaute[a*], Cécile Sicard-Roselli[b*]

Received ooth January 2012,
Accepted ooth January 2012

DOI: 10.1039/xoxxoooooox

www.rsc.org/

Electron transfer inside proteins plays a central role in their reactivity and biological functions. Herein, we developed a combined approach by gamma radiolysis and electrochemistry which allowed a deep insight into the reactivity of Human centrin 2, a protein very sensitive to oxidative stress and involved in several key biological processes. This protein bears a single terminal tyrosine and was observed to be extremely sensitive to ionizing radiations, leading to a tyrosine dimer. By cyclic voltammetry in the 100-1000 Vs^{-1} range, its redox potential and dimerization rate could be evaluated. Accordingly, reaction in solution with a redox mediator revealed an efficient catalysis. Finally, the protein denaturation by a progressive increase in temperature was proportional to a decrease of dimerization radiolytic yield. Our results thus demonstrated that the protein structure plays a major role in the oxidation sensitivity. This leads to meaningful results to understand protein redox reactivity.

Introduction

The way the protein core affects the chemical reactivity of a specific site is a central question of modern biophysical chemistry. For example, even if enzymatic reactions are most often performed by an "active site", the whole enzyme pocket is crucial for selectivity and has also an influence on the activation barrier.[1-3] The same question of the protein core influence arises for redox systems, where electron transfer(s) is (are) possibly coupled to proton exchange(s).[4, 5] A wide number of small synthetic biomimetic systems have been investigated either by photochemical or electrochemical methods.[6-10] Nevertheless, electrochemical investigations usually require submillimolar concentrations and several milliliters of solution, conditions not often accessible for proteins. In addition, for large systems, electrode passivation often hinders in-depth mechanistic studies and often requires specific tailoring of the interface.[11, 12]

Another alternative to induce redox processes in biological systems stems from radiolysis[13-18] which allows to produce specifically and quantitatively oxidative or reductive species.[19, 20] In this context of increasing interest for redox properties of proteins, we address in this paper electrochemical and radiolytic investigations onto Human centrin 2 (Hscen2), a protein that belongs to the calciprotein superfamily. It is implicated in important biological processes such as DNA nucleotide excision repair[21-23] and cell division.[24] Hscen2 is a 20 kDa two-domain acidic protein of 172 amino-acids. Structural studies by X-ray crystallography and NMR allowed to determine almost all the structure of Hscen2 and revealed that it includes seven alpha-helices.[25-28] Most important for redox properties, it contains a single tyrosine (Tyr 172) in terminal position but no tryptophan nor cysteine so that redox reactions mainly concern Tyr 172.

It has been demonstrated that oxidative stress agents[29, 30] or ionizing radiations[31] induce centrosome functioning abnormalities, and Hscen2 seems to be linked to centrosome defects.[32, 33] Identifying the exact impact of oxidative species onto Hscen2 appears then very important. This work brings new features about the radiolytic sensitivity of Hscen2 in complement with previous studies and for the first time explores also the electrochemical behavior of this protein. In the following, we first compare the radiosensitivity of Hscen2 with isolated tyrosine using a radiolytic approach. Then, we oxidize the protein by electrochemical methods, either directly at the electrode or by redox catalysis. Finally, we follow concomitantly protein unfolding and reactivity as a function of temperature.

Results and discussion

γ irradiation of Hscen2 and tyrosine

Reactive oxygen species (ROS) such as hydroxyl radicals $HO^{\bullet}$ can be produced *ex vivo* by radiolysis. This radical is nevertheless poorly selective as its redox potential is extremely high (2.78 V vs SHE)[34, 35] which allows electron transfer onto numerous aminoacids. Moreover, it can also induce radical reactions such as H abstraction or addition.[34] To better control the reactive paths, the $N_3^{\bullet}/N_3^-$ system having a much lower redox potential (1.31 vs SHE) can also be used.[15, 16] For that,

the primary species produced by water radiolysis need to be scavenged to form azide radicals as described in scheme 1.[36, 37] Indeed, electrons and hydrogen atoms react with N_2O to produce $HO^\bullet$ that further attacks N_3^- to finally produce $N_3^\bullet$.

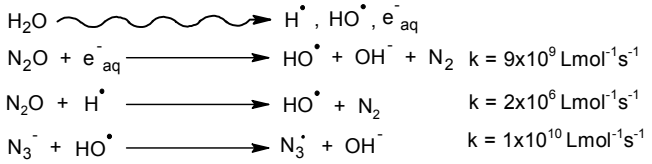

Scheme 1. Radical reaction cascades induced by γ irradiation of an aqueous solution containing N_2O and N_3^- and corresponding rate constants.

In former studies, Hscen2 oxidation was shown to lead to dimers and other higher molecular mass species, dimer formation being largely favored for lower doses. Mass spectrometry revealed that resulting dimers are formed from covalent bonding between C-terminal tyrosine Tyr 172 residues of each monomer, at α position from hydroxyl group. The same coupling was previously described by Sharma and Jain for an isolated tyrosine.[38] This suggested a mechanism for which one electron and one proton are removed from Hscen2, followed by a dimerization of the neutral radical. Thus, as expected for $N_3^\bullet$,[39] the tyrosinyl residue is the preferential site of oxidative attack of the protein.[16] Methionine entities inside proteins have a much larger redox potential (above 1.4 V vs SHE)[40, 41] than tyrosine and only Met19 was shown to be a sensitive minor site of oxidation. Interestingly, Hscen2 was shown to be sensitive to much lower oxidative radical concentrations than other proteins.[42, 43]

For a complete comparison with previous investigations, we performed here similar irradiations for tyrosine and Hscen2. They were submitted to γ irradiation in phosphate buffer at pH 7.0 and oxidized by $N_3^\bullet$.

As previously observed, radiolytic oxidation led to the formation of dityrosines. Reactant consumption and products apparition were measured differently according to the sample. Reaction products were quantified by HPLC for isolated Tyr. Hydrophobic separation showed that in addition to tyrosine signal, a dimer and for higher doses a trimer, were formed as already reported.[15, 44] Integration of the 280 nm absorption signal, taking into account the molar extinction coefficients already determined,[16, 45] allowed us to quantify tyrosine disappearance and dimer formation. For Hscen2 these analysis were performed by integrating gel electrophoresis signals of monomeric and dimeric centrins.[17]

The radiolytic yields are a direct measurement of reactant consumption and product apparition. We measured the yield of disappearance of Hscen2 and tyrosine and obtained: $G_{(-Hscen2)}$ = 0.57± 0.05 μmolJ^{-1} and $G_{(-Tyr)}$ = 0.27 ± 0.04 μmolJ^{-1} (see figure S1a in ESI) which surprisingly suggests that Hscen2 may be more reactive than tyrosine. Respective dimer formation yields were $G_{(Hscen2Dimer)}$ = 0.26 ± 0.02 μmolJ^{-1} and $G_{(TyrDimer)}$ = 0.046 ± 0.002 μmolJ^{-1} (see figure S1b). These results point out first the great difference between both samples and second the higher sensitivity of Hscen2 towards oxidation. In addition, since $G_{(Hscen2Dimer)}$ is almost half $G_{(-Hscen2)}$, dimerization is the only radical pathway for Hscen2, which is not the case for tyrosine, suggesting the presence of other oxidation by-products not detected in our conditions. Since redox potentials for tyrosine is well below the one of $N_3^\bullet/N_3^-$, we suggested that the initial tyrosine may be formed back from the radical through reaction with one of those products. Observing a stronger sensitivity for a much larger entity despite possible steric constraints appears very counterintuitive. Therefore, we examined the redox behavior of Hscen2 in comparison with tyrosine from a molecular electrochemical approach in order to examine the influence of thermodynamic (standard potential) and kinetic (rate constants) parameters onto the global reactivity.

Direct electrochemistry

One of the simplest way to measure the redox potential of an unstable intermediate is to get a reversible wave in cyclic voltammetry.[46, 47] Despite the difficulty of extracting voltammetric signals with natural proteic systems without specific engineering of the system or the interface,[11, 48] we attempted to oxidize Tyr 172 directly at the electrode surface. In fact, we obtained no signal for Hscen2 at 0.2 mM concentrations with glassy carbon or platinum electrodes. Surprisingly, as depicted in figure 1 and figure S2, for Hscen2, a backward peak was obtained on a gold microelectrode (diameter 125 μm) when increasing the scan rate v above 100 Vs^{-1}. This could highlight a specific interaction of Hscen2 with gold. As ten methionine residues are present along Hscen2 sequence, they could be responsible for strong interactions between the protein and the gold electrode surface.[49] Nevertheless, even if the redox potential of methionine may be affected by the protein structure,[41] it remains probably too high to induce a faradaic current in the potential window explored by cyclic voltammetry. These voltammograms present clear reversible behavior showing Hscen2 radicals that were stable during the time scale of cyclic voltammetry (on the order of RT/(Fv)).

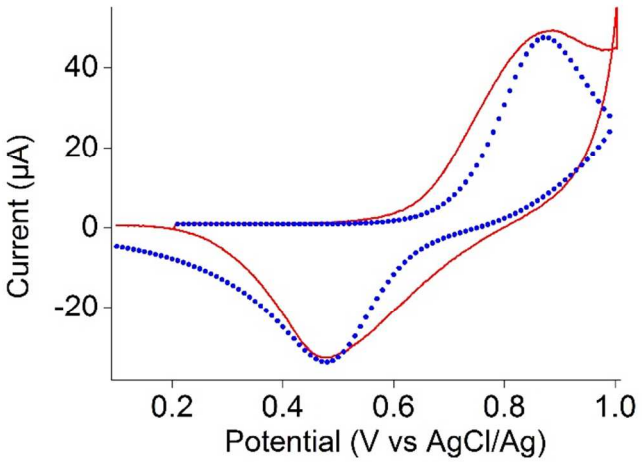

Figure 1. Cyclic voltammograms at 1000 Vs^{-1} in water containing 0.2 mM Hscen2 + 0.2 M NaCl on a 125 μm diameter gold microelectrode. Experimental (red solid line) and simulated (blue circles) currents. The background current is subtracted. Simulation parameters: E^0 = 0.675 V vs AgCl/Ag diffusion coefficient D_{Hscen2} = 8.2x10^{-7} cm^{2}s^{-1}, k_{dim} = 4.5x10^3 Lmol^{-1}s^{-1}, layer thickness = 180 nm, [Hscen2] = 65 mM. pH = 7.5.

Conversely, for tyrosine we could not obtain any reversibility of the signal in cyclic voltammetry (see figure S3). As expected for low concentrations, the background signal (proportional to v) becomes predominant over the faradaic one (proportional to $v^{1/2}$) for scan rates larger than 100 Vs^{-1}, hindering any reversibility observation. This demonstrated a much smaller lifetime of the free tyrosine radical. By pulse radiolysis, some

of us measured indeed a fast dimerization rate of $5x10^8$ $Lmol^{-1}s^{-1}$.[50] This rate is slightly lower but in line with what was demonstrated at neutral medium for phenolic compound oxidation which involves a one-electron one proton loss followed by a fast dimerization rate evaluated to ca. $1.3x10^9$ $Lmol^{-1}s^{-1}$ which was very close to the diffusion limit.[51] These results testify for the higher radical stability in the case of the protein compared to isolated tyrosine.

For Hscen2, a quantitative analysis reveals that the current densities were much higher than what can be expected for a 0.2 mM concentration of the protein. The possibility that the signal stemmed only from a single adsorbed monolayer could be excluded since then unrealistic molecular coverages, much higher than what can be expected from the size of Hscen2 (roughly a cylinder with a 3 nm diameter and 6.6 nm height), would need to be introduced. Any contribution from the background current or direct gold oxidation could also be excluded since there was no faradaic signal using a blank solution without Hscen2. This suggested that a more concentrated layer of proteins was present at the electrode surface.

Electrochemical simulations were in agreement with experimental data considering a 180 nm thick protein layer. The estimated concentration determined for this layer was 65 ± 5 mM. Accordingly, these simulations justify the absence of any signal at low scan rates. We were concerned by the fact that Hscen2 tends to make non-covalent aggregates in high ionic strength solutions.[25] We thus explored the behavior of Δ25centrin2. This protein is very similar to Hscen2 except that the first 25 residues are removed. The lack of these amino acids prevents this protein from aggregation in the bulk solution but the final tyrosine residue is still active towards oxidation.[15] Nevertheless, a similar trend to film formation on the gold surface was observed, with film thickness and concentrations of respectively 180 nm and 59 ± 5 mM. Experimental and simulated cyclic voltammograms are presented in figures S4 and S5. This observation suggest that non-covalent centrin aggregates and consequently N-terminal residues are not the cause of film formation on the electrode.

Our hypothesis is then that even if we checked that in the bulk the solution is still homogeneous, a film could be formed onto the electrode surface. Electrochemical simulations led to a value of $E°_{app}$ =675 ± 20 mV vs AgCl/Ag for Hscen2 apparent redox potential. Literature reports an apparent redox potential for tyrosine of about 730 mV vs AgCl/Ag.[52, 53] Supposing the same oxidation mechanism for radiolysis and electrochemistry (*i.e.* one electron oxidation and dimerization of tyrosinyl residue), it seemed that the tyrosinyl residue from Hscen2 had a lower oxidation potential than tyrosine itself. Such effect has already been observed for short peptides and proteins incorporating tyrosine entities[52] but such slight difference could nevertheless not explain the difference of reactivity compared to tyrosine. In agreement with observation of reversibility in the 100-1000 Vs^{-1} range and the concentration inside the film, the dimerization rate constant is estimated to be k_{dim} = 4.5 ± $1x10^3$ $M^{-1}s^{-1}$, thus much smaller than the nearly diffusion limited value estimated for tyrosine. In order to react, both radicals should indeed be in close proximity. It is likely that sterical constraints due either to the film or to rotational diffusion prevented a favorable orientation of tyrosinyl residues, justifying such slow reactivity as already proposed.[15]

This section presented for the first time that within Hscen2, the tyrosine moiety kept its electroactivity with a smaller but close standard potential compared to tyrosine which is a first important indication. Nevertheless, the peculiar conditions into which reversible voltammograms were obtained required the use of complementary observations by redox catalysis for which electron transfer occurs in the bulk solution in a similar manner compared to radiolysis.

Insights from redox catalysis

Homogeneous redox catalysis was then used to gain further insight about reactivity of Hscen2 in solution. In this technique, a redox mediator, here $Os(bipy)_3^{2+}$ was oxidized at the electrode. It further reacted in solution with Hscen2 to regenerate the original reduced form of the mediator that could start another cycle. The current amplification is therefore directly correlated with the reaction rate. For that purpose, we used Indium Tin Oxide (ITO) electrodes for which phosphate adsorption totally blocks the direct electron transfer from Hscen2.[9, 10] $Os(bipy)_3^{2+}$ could nevertheless be quantitatively oxidized and mediate electron transfer towards Hscen2 according to scheme 2:[46]

$$Os(bipy)_3^{2+} - e^- \rightleftharpoons Os(bipy)_3^{3+}$$
$$Os(bipy)_3^{3+} + \text{Hscen2} \xrightarrow{k_{app}} Os(bipy)_3^{2+} + \text{Products}$$

Scheme 2. Redox catalysis of Hscen2 oxidation.

Figure 2 presents the voltammograms obtained for a solution containing 11 µM $Os(bipy)_3^{2+}$ and 100 µM Hscen2 at different buffer concentrations. Efficient regeneration of the catalyst at the electrode is evidenced by a current increase with buffer concentration and loss of reversibility of the oxidation wave. We observed that the catalytic rate depends on the buffer concentration for a constant pH.

Within the simplified analysis in the frame of scheme 2, we could even determine by digital simulations the apparent catalytic rate constant k_{app}, relying on the redox potential determined for Hscen2 in the previous section. We found respectively k_{app} = (6.9 ± 0.2)$x10^4$, (9.8 ± 0.2)$x10^4$ and (1.7 ± 0.2)$x10^5$ $Lmol^{-1}s^{-1}$ for 10, 50 and 100 mM buffer concentration. The excellent fits obtained in figure 2 validated our analysis.

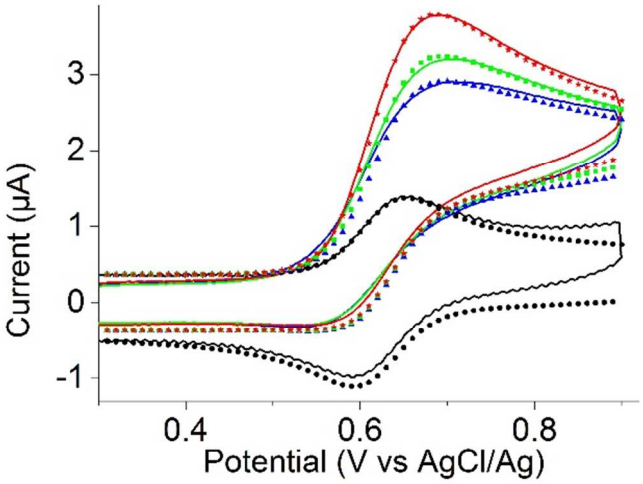

Figure 2. Experimental cyclic voltamograms of 11 µM $Os(bpy)_3^{2+}$ (black solid line) and in the presence of 0.1 mM Hscen2 with 10 mM (blue), 50 mM (green) and 100 mM (red) of phosphate buffer at pH 7.5 in 0.1 M NaCl aqueous solution. An ITO electrode was used in order to block direct electron transfer. Scan rate 100 mVs^{-1}. Symbols:

corresponding simulated cyclic voltammograms.

We also performed a similar experiment with tyrosine as reported in figure S6. We observed larger catalytic currents in that case. The sole consideration of a larger diffusion coefficient for tyrosine could not explain the 4-5 fold current enhancement compared to Hscen2. Tyrosine oxidation mechanism has already been deeply studied by Fecenko *et al.* who also used homogeneous redox catalysis with various electrochemical mediators.[9, 10] They concluded that homogeneous oxidation of tyrosine occurs in two steps: (1) association of tyrosine with the base form of the buffer (presumably *via* H-bonding) (2) the formed complex can react either *via* concerted loss of electrons and protons or *via* rate-limiting proton transfer followed by electron transfer. Conversely, Saveant and co-workers examined phenol oxidation in buffered or not media and found a concerted mechanism.[4, 7] We believe in fact that when buffer concentration is high, proton transfers are probably at equilibrium so that variation of the reaction rate at fixed pH and driving force indicated a concerted path.

With Hscen2 the current increased with buffer concentration, but still remained much smaller than the one measured for tyrosine. This trend suggested again that the protein backbone may stabilize tyrosinyl radical, avoiding side reactions and justifying agreement between Hscen2 consumption and dimer apparition at low doses. This would explain a small assistance by the buffer which is possibly here replaced by the protein. Our analysis also revealed that electron transfer between Os^{III} and Hscen2 could be followed or concerted with an irreversible reaction, probably the proton exchange. Indeed, for an efficient redox catalysis, there must be a fast (and even better irreversible) reaction to pull electron transfer. Even if here the dimerization rate may be larger than determined in the previous section, we did not expect it to vary by several orders of magnitude so as to drive the catalysis. The rate determining step then occurred necessarily prior to dimerization.

Influence of temperature.
In order to confirm the important role of the protein backbone in the reaction, we determined the dimerization yield of Hscen2 as a function of its secondary structure. This was performed by increasing the temperature that induces a loss of alpha helices content in Hscen2 as confirmed by circular dichroism. Figure S7 and figure 3 revealed a linear decrease of alpha helix content with the temperature indicating a progressive unfolding. Considering a native structure at 5°C, Hscen2 lost 60 % of alpha helices at 80°C which proved its high temperature resistance compared to other proteins.[54] In parallel, we also followed the percentage of dimer yield formation ($G_{(Hscen2Dimer)}/2G(_{-N3}\bullet)$) with temperature, and found that it matched the circular dichroism data, as evidenced in figure 3. Therefore, it seems that a loss of structure increased the degree of side reactions.
This suggested a very important role of proximal amino-acids. Nevertheless, from X-Ray or NMR protein structure it was not possible to point out the residues implicated as the centrin C-terminal Tyr residue is in a very flexible region.[26-28] Hence, this experiment confirmed the crucial role of the whole protein structure and hydrogen bonds on Tyr 172 reactivity suggesting again that proton transfers could also play a key role in the electron transfer mechanism.

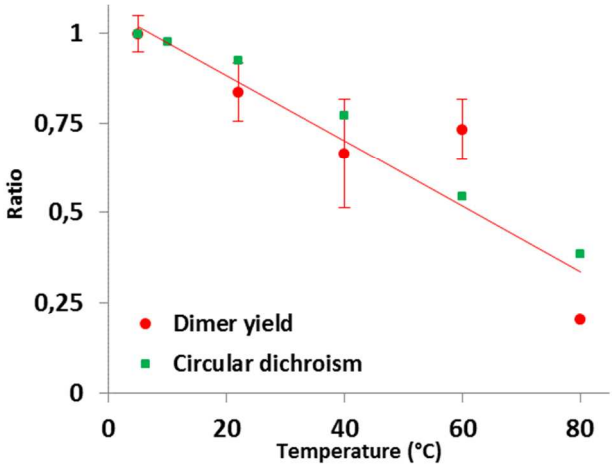

Figure 3. Comparison of dimerization yield and unfolding of Hscen2. Dimer yield corresponds to the ratio $G_{(Hscen2Dimer)}/2G(_{-N3}\bullet)$ for each temperature and was divided by the value obtained at 5°C. Circular dichroism ratio is the percentage of alpha helices content (signal at 222 nm) considering 100% at 5°C. pH = 7.0. Straight line represents a linear fit of the dimer yield.

Conclusions

Extracting mechanistic information onto large native biological systems is often tricky because many reaction pathways can be simultaneously activated leading to a large number of products. In this way, Hscen2 appeared as a model system since a single product, a tyrosine dimer could be identified upon oxidation. It was produced stoechiometrically with azide radical, a mild oxidant. For the same irradiation dose, more dimer was produced compared to isolated tyrosine. The dimer yield decreased as the protein was denatured by a temperature increase. Those results pointed out the major influence of the protein structure for the redox reactivity and selectivity. They also reinforce the idea of a peculiar role of this protein towards biological oxidative stress agents. By transient electrochemistry, we measured a slightly lower standard potential compared to tyrosine but a much slower chemical coupling between the radicals. Such low difference between redox potentials could however not explain solely the differences observed for both systems. We also observed an efficient redox catalysis further confirming the reactivity of Hscen2. It may seem surprising to detect a larger sensitivity despite a lower reactivity. However, with tyrosine, radical reactivity is less oriented so that several products are formed, and among them the starting tyrosine. Conversely, we propose that Hscen2 radicals are stabilized but still reactive. The reaction would then be directed towards a single reaction path, here a dimerization. These major deductions could be achieved thanks to an unprecedented methodology combining gamma radiolysis and electrochemistry. In the future, other biological systems may benefit from such combined approach.

Experimental

Human centrin 2 (total and Δ25) production in *E. Coli* and purification were already described previously.[15]
To quantify tyrosine dimer formation, chromatographic experiments were performed on an HPLC (Beckman 168) in reverse phase (Kromasil C18 5µm 250x4.6 mm) with a gradient

between two elution buffers A (0.1% TFA) and B (0.1% TFA, 70% acetonitrile). The samples were submitted to the following gradient with a 1 $mLmin^{-1}$ flow rate: 0% B during 5 min, 0-30% B in 5 min, 30-50% B in 20 min, 50-100% B in 5 min. The absorbance was simultaneously recorded at 214 and 280 nm.

For radiolysis experiments, 50 µM tyrosine or centrin solutions were prepared in 10 mM phosphate buffer at pH 7.0. All samples were flushed with N_2O gas for one hour, avoiding bubbling in the solution, in order to obtain a complete saturation of the samples. To provide azide radicals, 10 mM NaN_3 was added to the buffer.

Gamma radiolysis experiments were performed on a panoramic ^{60}Co source (IL60PL Cis-Bio International). Doses were determined with a Fricke dosimeter[37] taking into account the container used to maintain the desired temperature (water or sand bath). The dose rate was 2 $Gy.min^{-1}$. Also, temperature changes were taken into account to determine the radical yield of formation.

Circular dichroism spectra of 0.1 $mgmL^{-1}$ of Hscen2 samples in 10 mM sodium phosphate pH = 7.4 were recorded from 5°C to 80°C with a J-710 Jasco spectrometer continuously purged with N_2 and equipped with a Peltier temperature controller. The cell optical path was 1 mm. Each spectrum corresponds to the average of three scans recorded between 185 and 250 nm. Spectrum of the buffer alone was also recorded in the same conditions for each temperature and subtracted to Hscen2 dichroic spectra. To quantify dimer formation, SDS-PAGE electrophoresis was run on 12% acrylamide-bisacrylamide gels with a Tris-Tricine buffer under non–reducing conditions. 10 µg of protein were deposited in each well of the gels. Staining was done with Coomassie Blue R-250 according to standard procedures.

Electrochemical experiments were carried out using Autolab PGSTAT 100. The electrochemical cell volume was 500 to 1000 µL. The working electrode was a 125 µm diameter circular-shaped gold microelectrode for cyclic voltammetry and a 0.44 cm^2 ITO electrode for homogeneous catalysis redox experiments. A small home-made AgCl/Ag in a 3M KCl agar-agar gel was used as reference electrode, excepted for direct electrochemistry with tyrosine for which we resorted to a commercial saturated calomel electrode (SCE) All reference electrodes were calibrated versus a specific SCE used only for calibration prior experiment. A platinum wire was used as reference and counter electrodes. The supporting salt was NaCl at a concentration of 0.2M for cyclic voltammetry and 0.1M for homogeneous redox catalysis. Hscen2 concentrations were 0.2 mM and 0.1 mM for cyclic voltammetry and homogeneous catalysis redox experiments, respectively. It is important to note that electrochemistry requires higher protein concentrations compared to radiolysis experiments in order to get correct signal/noise ratios. Therefore, the available amount of Hscen2 did not allow a large number of experiments which had to be chosen carefully and realized quickly as the protein keeps in a stable state in buffer solutions only for few hours. $Os(bpy)_3^{2+}$ was synthesized using published procedures.[55] Simulations were realized using the commercial software DigiElch Professional. Since diffusion coefficient of Hscen2 is not available to the best of our knowledge, we relied on the one determined by a new NMR technique for a protein of similar molecular weight: $8.2x10^{-7}$ cm^2s^{-1}.[56]

Acknowledgements

This work was supported by ANR, the French national research agency (project Radiolyse et Analyse Dynamique par Electrochimie, JCJC 0810). We thank Dr. Damien Laage and Dr. Fabien Ferrage (Ecole Normale Supérieure) and Pr. Marc Robert (Université Paris-Diderot) for helpful discussions. We acknowledge Dr. Claire Fave and Pr. Bernd Schöllhorn (Université Paris-Diderot) for their help in the synthesis of the Os complex.

Notes and references

[a] Sorbonne Universités, UPMC Univ Paris 06, UMR 8235, Laboratoire Interfaces et Systèmes Electrochimiques, F-75005, Paris (France).
[b] Laboratoire de Chimie Physique, CNRS UMR 8000, Université Paris 11, Bât. 350, 91405 Orsay Cedex, France.
[c] Plateforme Production Protéines Recombinantes, Institut Curie - INSERM U759, Université Paris-Sud, 91405 Orsay Cedex.
[d] Institut Curie - INSERM U759, Université Paris-Sud, 91405 Orsay Cedex.
[e] Institut UTINAM, CNRS UMR 6213, Université de Franche-Comté, 30 avenue de l'Observatoire, 25009 Besançon Cedex, France.

1. J. Stubbe, D. G. Nocera, C. S. Yee and M. C. Y. Chang, *Chem. Rev.*, 2003, 103, 2167-2201.
2. S. J. Benkovic and S. Hammes-Schiffer, *Science*, 2003, 301, 1196-1202.
3. A. C. Fogarty, E. Duboue-Dijon, F. Sterpone, J. T. Hynes and D. Laage, *Chem. Soc. Rev.*, 2013, 42, 5672-5683.
4. C. Costentin, C. Louault, M. Robert and J. M. Saveant, *Proc. Natl. Acad. Sci. USA*, 2009, 106, 18143-18148.
5. C. Costentin, M. Robert and J. M. Saveant, *Accounts Chem. Res.*, 2010, 43, 1019-1029.
6. J. Bonin, C. Costentin, M. Robert, M. Routier and J. M. Saveant, *J. Am. Chem. Soc.*, 2013, 135, 14359-14366.
7. C. Costentin, C. Louault, M. Robert and J. M. Saveant, *J. Am. Chem. Soc.*, 2008, 130, 15817-15819.
8. M. Sjodin, R. Ghanem, T. Polivka, J. Pan, S. Styring, L. C. Sun, V. Sundstrom and L. Hammarstrom, *Phys. Chem. Chem. Phys.*, 2004, 6, 4851-4858.
9. C. J. Fecenko, T. J. Meyer and H. H. Thorp, *J. Am. Chem. Soc.*, 2006, 128, 11020-11021.
10. C. J. Fecenko, H. H. Thorp and T. J. Meyer, *J. Am. Chem. Soc.*, 2007, 129, 15098-15099.
11. C. Leger and P. Bertrand, *Chem. Rev.*, 2008, 108, 2379-2438.
12. P. Fortgang, E. Maisonhaute, C. Amatore, B. Delavaux-Nicot, J. Iehl and J. F. Nierengarten, *Angew. Chem.-Int. Edit.*, 2011, 50, 2364-2367.
13. M. H. Klapper and M. Faraggi, *Q. Rev. Biophys.*, 1979, 12, 465-519.
14. P. Wardman, *Br. J. Radiol.*, 2009, 82, 89-104.
15. Y. Blouquit, P. Duchambon, E. Brun, S. Marco, F. Rusconi and C. Sicard-Roselli, *Free Radic. Biol. Med.*, 2007, 43, 216-228.
16. E. Brun, Y. Blouquit, P. Duchambon, C. Malosse, J. Chamot-Rooke and C. Sicard-Roselli, 2010, 86, 657-668.
17. J. Cadet, T. Douki and J. L. Ravanat, *Accounts Chem. Res.*, 2008, 41, 1075-1083.
18. A. Harriman, *J. Phys. Chem.*, 1987, 91, 6102-6104.
19. C. Ferradini and J.-P. Jay-Gerin, *Can. J. Chem.*, 1999, 77, 1542-1575.
20. J. A. LaVerne, *Radiat. Res.*, 2000, 153, 196-200.

21. R. Nishi, Y. Okuda, E. Watanabe, T. Mori, S. Iwai, C. Masutani, K. Sugasawa and F. Hanaoka, *Mol. Cell Biol.*, 2005, 25, 5664-5674.
22. R. Nishi, W. Sakai, D. Tone, F. Hanaoka and K. Sugasawa, *Nucleic Acids Res.*, 2013, 41, 6917-6929.
23. C. N. Cunningham, C. A. Schmidt, N. J. Schramma, M. R. Gaylord and K. K. Resendes, *Exp. Cell Res.*, 2014, 320, 209-218.
24. J. L. Salisbury, *Curr. Opin. Cell. Biol.*, 1995, 7, 39-45.
25. M. Tourbez, C. Firanescu, A. Yang, L. Unipan, P. Duchambon, Y. Blouquit and C. T. Craescu, *J. Biol. Chem.*, 2004, 279, 47672-47680.
26. A. Yang, S. Miron, P. Duchambon, L. Assairi, Y. Blouquit and C. T. Craescu, *Biochemistry*, 2006, 45, 880-889.
27. E. Matei, S. Miron, Y. Blouquit, P. Duchambon, I. Durussel, J. A. Cox and C. T. Craescu, *Biochemistry*, 2003, 42, 1439-1450.
28. J. R. Thompson, Z. C. Ryan, J. L. Salisbury and R. Kumar, *J. Biol. Chem.*, 2006, 281, 18746-18752.
29. S. Chae, C. Yun, H. Um, J. H. Lee and H. Cho, *Exp. Mol. Med.*, 2005, 37, 482-487.
30. H. Loffler, A. Fechter, F. Y. Liu, S. Poppelreuther and A. Kramer, *Oncogene*, 2013, 32, 2963-2972.
31. N. Sato, K. Mizumoto, M. Nakamura, H. Ueno, Y. A. Minamishima, J. L. Farber and M. Tanaka, *Oncogene*, 2000, 19, 5281-5290.
32. J. J. Li, S. J. Weroha, W. L. Lingle, D. Papa, J. L. Salisbury and S. A. Li, *Proc. Natl. Acad. Sci. USA*, 2004, 101, 18123-18128.
33. W. L. Lingle, W. H. Lutz, J. N. Ingle, N. J. Maihle and J. L. Salisbury, *Proc. Natl. Acad. Sci. USA*, 1998, 95, 2950-2955.
34. C. Von Sontag, *Free-radical-induced DNA damage and its repair. A chemical perspective*, Springer, Berlin, 2006.
35. E. Sutter, K. Jungjohann, S. Bliznakov, A. Courty, E. Maisonhaute, S. Tenney and P. Sutter, *Nat. Commun.*, 2014, 5.
36. M. R. Defelippis, M. Faraggi and M. H. Klapper, *J. Phys. Chem.*, 1990, 94, 2420-2424.
37. J. W. T. Spinks and R. J. Woods, *Introduction to radiation chemistry*, Wiley, New-York, third edn., 1990.
38. M. Sharma and R. Jain, *Chem.-Biol. Interact.*, 1998, 108, 171-185.
39. M. Weinstein, Z. B. Alfassi, M. R. Defelippis, M. H. Klapper and M. Faraggi, *Biochim. Biophys. Acta*, 1991, 1076, 173-178.
40. W. A. Prutz, J. Butler, E. J. Land and A. J. Swallow, *Int. J. Radiat. Biol.*, 1989, 55, 539-556.
41. P. Brunelle and A. Rauk, *J. Phys. Chem. A*, 2004, 108, 11032-11041.
42. C. Sicard-Roselli, S. Lemaire, J. P. Jacquot, V. Favaudon, C. Marchand and C. Houee-Levin, *Eur. J. Biochem.*, 2004, 271, 3481-3487.
43. J. Arvieux, V. Regnault, E. Hachulla, L. Darnige, F. Berthou and P. Youinou, *Thromb. Haemostasis*, 2001, 86, 1070-1076.
44. T. G. Huggins, M. C. Wells-Knecht, N. A. Detorie, J. W. Baynes and S. R. Thorpe, *J. Biol. Chem.*, 1993, 268, 12341-12347.
45. D. A. Malencik, J. F. Sprouse, C. A. Swanson and S. R. Anderson, *Anal. Biochem.*, 1996, 242, 202-213.
46. J.-M. Saveant, *Elements Molecular and Biomolecular Electrochemistry*, John Wiley and Son, Hoboken, New Jersey, first edn., 2006.
47. C. Amatore, G. Farsang, E. Maisonhaute and P. Simon, *J. Electroanal. Chem.*, 1999, 462, 55-62.
48. B. W. Berry, M. C. Martinez-Rivera and C. Tommos, *Proc. Natl. Acad. Sci. USA*, 2012, 109, 9739-9743.
49. E. Cooper, F. Krebs, M. Smith and R. Raval, *J. Electron Spectrosc. Relat. Phenom.*, 1993, 64-5, 469-475.
50. C. Sicard-Roselli, personal communication.
51. L. Papouchado, R. W. Sandford, G. Petrie and R. N. Adams, *J. Electroanal. Chem.*, 1975, 65, 275-284.
52. M. R. Defelippis, C. P. Murthy, F. Broitman, D. Weinraub, M. Faraggi and M. H. Klapper, *J. Phys. Chem.*, 1991, 95, 3416-3419.
53. M. R. Defelippis, C. P. Murthy, M. Faraggi and M. H. Klapper, *Biochemistry*, 1989, 28, 4847-4853.
54. S. R. Tello-Solís and B. Romero-García, *Int. J. Biol. Macromol.*, 2001, 28, 129-133.
55. C. Creutz, M. Chou, T. L. Netzel, M. Okumura and N. Sutin, *J. Am. Chem. Soc.*, 1980, 102, 1309-1319.
56. R. Augustyniak, F. Ferrage, C. Damblon, G. Bodenhausen and P. Pelupessy, *Chem. Commun.*, 2012, 48, 5307-5309.

Human centrin 2 is a protein very sensitive to oxidative stress. Protein reactivity is unraveled by gamma radiolysis and electrochemical techniques.